NASA Technical Memorandum 79147

A COMPARISON OF MEASURED AND CALCULATED UPWELLING RADIANCE OVER WATER AS A FUNCTION OF SENSOR ALTITUDE

Thom A. Coney and Jack A. Salzman
Lewis Research Center
Cleveland, Ohio

Prepared for the
Thirteenth International Symposium on
Remote Sensing of Environment
sponsored by the University of Michigan
Ann Arbor, Michigan, April 23-27, 1979

A COMPARISON OF MEASURED AND CALCULATED UPWELLING RADIANCE OVER WATER AS A FUNCTION OF SENSOR ALTITUDE

Thom A. Coney, and Jack A. Salzman

NASA-Lewis Research Center
Cleveland, Ohio

SUMMARY

A comparison is made between remote sensing data measured over water at altitudes ranging from 30 m to 15.2 km and data calculated for corresponding altitudes using surface measurements and an atmospheric radiative transfer model. Data were acquired on June 22, 1978 in Lake Erie, a cloudless, calm, near haze free day. Suspended solids and chlorophyll concentrations were 0.59±0.02 mg/l and 2.42±0.03 μg/l respectively throughout the duration of the experiment. Remote sensor data were acquired by two multispectral scanners each having 10 bands between 410 nm and 1040 nm. Calculated and measured nadir radiances for altitudes of 152 m and 12.5 km agree to within 16% and 14% respectively. The variation in measured radiance with look angle was poorly simulated by the model. It was concluded that an accurate assessment of the source of error will require the inclusion in the analysis of the contributions made by the sea state and specular sky reflectance.

E-003

INTRODUCTION

Although various water quality parameters have been successfully measured using remote sensing techniques, there are a number of problems which must be solved before such techniques can be employed in operational monitoring. Theoretical and laboratory studies, as well as field experiments, have demonstrated that concentrations of chlorophyll, suspended solids and other substances in the water can be interpreted from measurements of the intrinsic water color (refs. 1 and 2). While there is still work needed to quantify and expand these interpretative capabilities, of equal necessity is the development of techniques to accurately measure the water color from remote platforms. Aperture radiance values measured by remote sensors contain the necessary surface water color data but perturbations due to atmospheric interactions make their accurate extraction quite complex. Having the capability to correct for these atmospheric effects is essential before the unique perspective of satellite and aircraft systems and all their inherent advantages can be fully utilized.

Several theoretical models and computer programs have been developed to perform atmospheric corrections on remotely sensed data (refs. 3 and 4) but a major factor limiting their refinement and verification has been the lack of a suitable data base with which to compare model calculations. During the summer of 1978, the NASA Lewis Research Center organized a field experiment to acquire such data. These data have subsequently been used to test and refine an available atmospheric radiative transfer model (ref. 5) in order to evaluate its predictive capabilities. Other participants in this experiment included the U.S.

Environmental Protection Agency and Scripps Institute of Oceanography. Radiance data were acquired at altitudes ranging from 30 m (100 ft) to 15.2 km (50,000 ft) using two aircraft/multispectral scanner remote sensing systems. Optical data were also acquired both directly above the water's surface and at several subsurface depths using a submersible spectroradiometer (owned and operated by Scripps). These data included the total downwelling irradiance and the upwelling radiance at three depths and the total downwelling irradiance in air. All measurements were made over a spectral range from 410 nm to 720 nm.

The atmospheric radiative transfer model used calculates the total downwelling irradiance, the transmittance and the path radiance as a function of altitude. The model includes the effects of multiple scattering by gases and particulates in the atmosphere and of absorption by ozone in the near ultraviolet and visible part of the spectrum. Measured inputs to the model include date, time, barometric pressure, site latitude and longitude, aircraft altitude, and atmospheric optical thickness. Estimated inputs include the aerosol phase function, ozone absorption, and standard aerosol optical depths above 5 km.

Model predictions were compared with data acquired both at the surface and over the full range of altitudes. Downwelling irradiance was compared directly with the surface measurements. The calculated upwelling radiances at the surface were compared with the aircraft scanner data by including model predictions of atmospheric attenuation, path radiance and sky reflectance.

THEORY

In the formulation used here, the basic equation of remote sensing is:

$$L(\tau,\lambda,\mu_o\phi_o) = L_o(\tau_o,\lambda,\mu_o,\phi_o)\ T(\tau,\lambda,\mu_o) + L_p(\tau,\lambda,\mu_o,\phi_o) \qquad (1)$$

where $L(\tau,\lambda,\mu_o,\phi_o)$ is the aperture radiance measured by the sensor, $L_o(\tau,\lambda,\mu_o,\phi_o)$ is the surface radiance, $T(\tau,\lambda,\mu_o)$ is the transmittance of the atmosphere and $L_p(\tau,\lambda,\mu_o,\phi_o)$ is the atmospheric path radiance. τ,λ,μ_o and ϕ_o are the optical depth, wavelength, cosine of the solar zenith and solar azimuth angle respectively. $T(\tau,\lambda,\mu_o)$ and $L_p(\tau,\lambda,\mu_o,\phi_o)$ are determined by the atmospheric radiative transfer model.

The radiative transfer model considered was developed by Dr. Robert Turner (ref. 5) under contract to Lewis Research Center. The model calculates the total downwelling irradiance, the transmittance and the path radiance for a plane-parallel, horizontally spatially homogenous, isotropic atmosphere as a function of altitude. The model includes the effects of multiple scattering by gases and particulates in the atmosphere and of absorption by ozone in the near ultraviolet and visible part of the spectrum. It is presently applicable to haze levels ranging from near fog conditions to the clearest possible atmosphere and the wavelengths between 400 nm and ≈2.2 m (with the exception of the strong absorption regions in the near IR).

The input variables can be separated into two categories, i.e., those that are estimated and those that are measured (see table I). Estimated values are used where a measurement would be difficult or where a variable is relatively constant. The model input format is such that a measured value can be used in place of an estimated value.

EXPERIMENT

Instrumentation

The remote sensing data used in this experiment was obtained with two multispectral scanners, a ten band ocean color scanner (OCS) and an eleven band modular multispectral scanner (M^2S). The ten bands on the OCS are between 425 and 795 nm and have 20 nm bandwidths. Its full and instantaneous fields of view are

90° and 0.258° respectively. Its design altitude is 12.5 km. The OCS is mounted in a wing pod on the General Dynamics F-106 shown in figure 1.

The first eight bands of M^2S are in the visible spectrum between 410 and 720 nm and have bandwidths of about 40 nm. Bands nine and ten are centered in the near infrared at 815 and 1040 nm and have bandwidths of 90 nm. The eleventh band is in the thermal IR at 11 μ. The full and instantaneous fields of view of the M^2S are 90° and 0.143° respectively. Its variable scan rate allow contiguous coverage at altitudes from 0.3 to 6.1 km (1,000 to 20,000 ft). The M^2S is mounted on the Convair C-131 shown in figure 2.

The ship shown in figure 3 is the Environmental Protection Agency's R/V Crockett. On-board facilities include a wet laboratory and a chemistry laboratory. This ship was used to obtain all surface truth data i.e., chlorophyll a, b, and c, phaeophytin, and suspended solids concentrations (ref. 6) as well as the optical properties of the water and the atmosphere. Using their submersible spectroradiometer (fig. 4) Scripps Institute of Oceanography measured the total surface downwelling irradiance, the subsurface total downwelling irradiance at three depths and the subsurface upwelling radiance at three depths; and used these data to calculate the surface upwelling radiance and the surface reflectance. The seven band solar radiometer shown in figure 5 was used to measure the optical thickness of the atmosphere.

Experiment Procedure

To evaluate the utility of an atmospheric scattering model as applied to remotely sensed data it is most desirable to conduct the experiment under the least complicating environmental conditions; a cloud free atmosphere with a constant aerosol content, calm seas, and a large water area of low and unchanging chlorophyll and suspended solids concentrations. These conditions were most nearly attained on June 22, 1978. The scene shown in figure 6 was recorded at 1454 hours at the experiment site 14 km off Cleveland in Lake Erie. The sky was clear over the lake with only slight haze present and the seas were relatively calm. The suspended solids and chlorophyll concentrations were low, averaging 0.59±0.02 mg/l and 2.42±0.03 μg/l throughout the day.

Acquisition of Remote Sensing Data

The direction and time of each aircraft flight line was determined by the orientation of the sun. Experience has shown that for solar zenith angles less than 40° the incidence of sun glitter from the wavelets increases significantly. To maximize available light however, data should not be obtained at zenith angles greater than 60°. These bounds established two windows on the 22nd of June (a morning window, 0845 to 1045 hours, and an afternoon window, 1625 to 1825 hours) during which all remote sensing data were acquired. The C-131 obtained data at altitudes ranging from 30 m to 3.05 km (100 to 10,000 ft). A total of 21 ship overpasses were flown. The F-106 obtained data at altitudes ranging from 152 m to 15.2 km (500 to 50,000 ft) for a total of 10 overpasses. In all cases data were obtained with the aircraft flying in the solar plane and with the sun aft.

Acquisition of Surface Truth Data

The sequence of measurements made by Scripps began at 0915 and continued to 1700 hours. The first measurement in the sequence was of the total downwelling irradiance made on deck with the submersible spectroradiometer (spectral range 410 to 710 nm) as shown in figure 4. The spectroradiometer was then submerged under its support buoy (fig. 7) and the downwelling irradiance at three depths was measured. The spectroradiometer was then inverted and the upwelling radiance at three depths was measured. These subsurface measurements were then used to calculate surface upwelling radiance and surface reflectance (ref. 7).

The sequence was repeated such that a total of four measurements of the surface irradiance and eight measurements of the surface radiance and surface reflectance were made. Optical thickness measurements were made with two solar radiometers (fig. 5) every half hour from 0830 to 1800 hours.

Water samples were obtained twice during each window and once before and once after solar noon (~1330 hr). Each time samples were obtained at three depths; 1 m below the surface, at the mid-Secchi depth and at the Secchi depth (~9 m).

RESULTS AND DISCUSSION

A total of 31 overflights, 40 optical thickness measurements, 6 chlorophyll and suspended solids concentration measurements, and 26 irradiance and radiance measurements (using the Scripps submersible spectroradiometer) were made between 0830 and 1800 hours. The purpose in acquiring this large amount of data was to establish the variability of each parameter throughout the day, to establish trends so that extrapolation in time was possible, and to acquire data at varying solar zenith and azimuth angles. The following results are applicable to the general state of the water and air on June 22 and to three representative sensor altitudes i.e., 12.5 km (41,000 ft), the design altitude of OCS; and 3.05 km (10,000 ft) and 152 m (500 ft), the two altitudes coincident to both sensors.

Using the Scripps measurements for L_o in eq. 1, nadir aperture radiances L were calculated for comparison with the 30 and 152 m altitude remote sensor data. At these low altitudes T is nearly 1.0 and L_p is small relative to L_o Therefore the effects of the atmosphere are considered minimal. Eleven comparisons were made. In all cases the measured nadir radiances exceeded the calculated radiances (shaded area in fig. 8). The difference was attributed to specular reflectance of skylight at the air-water interface. The remote sensing equation was thus modified by the addition of a specular reflectance term L_sT, i.e.,

$$L = L_oT + L_p + L_sT \qquad (2)$$

where L_s is here defined as $\rho_s E_s(\tau,\lambda,\mu_o)/\pi$. The specular reflectance ρ_s is assumed to be independent of time and wavelength. $E_s(\tau,\lambda,\mu_o)$ is the diffuse sky irradiance and is calculated by the atmospheric scattering model. Figure 8 identifies the three components making up the measured aperture radiance as a function of wavelength. These data were obtained at an altitude of 152 m at 1736 hours. Note that at some wavelengths the specular radiance L_s is comparable in magnitude to the surface radiance L_o.

An estimate of the specular reflectance for June 22 was obtained by substituting the radiances measured remotely from 30 and 152 m for L; the surface radiance measured by Scripps for L_o; and the calculated values for T, L_p and E_s into eq. 2 and solving for ρ_s. A value of 2.0±0.06% was obtained for the specular reflectance using a total of eleven low altitude data sets. This is consistent with accepted values for the specular reflectance. This value of the specular reflectance was used in all subsequent comparisons of measured and calculated radiance. An example of the calculated radiance for an altitude of 12.5 km and 0915 hours and the relative magnitudes of the components of eq. 2 are shown in fig. 9. Note the significant increase in the path radiance term.

COMPARISON OF CALCULATED AND MEASURED RADIANCE

The data from two representative altitudes and two solar zenith angles are presented in figures 10 and 11. The solid lines represent the measured nadir radiances and the symbols the calculated nadir radiances. The latter were based on the interpolated Scripps measurement of the upwelling radiance at the surface; on the transmittance, path radiance, and diffuse sky irradiance as de-

termined by the atmospheric scattering model; and on the estimated specular reflectance. The error, averaged over all bands, was 14% and 16% at 12.5 km and 152 m respectively. Since the error did not change significantly with an increase in altitude, it cannot necessarily be attributed solely to the model calculations. As presented in figures 10 and 11 there are four potential sources of error; the interpolation in time of the upwelling surface radiance as measured by Scripps; the estimate of the specular reflectance; the calculation of the transmittance and path radiance by the atmospheric scattering model; and the accuracy of the radiance measurement at altitude. For this experiment the error associated with the last three is relatively fixed. However, greater confidence in the results can be realized if the comparison is made between surface reflectances rather than between upwelling radiances.

Because of the technique used by Scripps to measure the upwelling surface radiance, the measurement is most accurate when made near solar noon (ref. 7). All remote sensor data however were obtained at times greater than 2 1/2 hours from solar noon. To minimize the error due to interpolation of surface radiance it is possible to consider the surface reflectance rather than an absolute measure of radiance. Surface reflectance is a function of water content but is nearly independent of time. Since the chlorophyll and suspended solids were constant throughout the day, the optimum single measure of surface reflectance (also at solar noon) can be used independent of the time. (Note: the calculated reflectance is strongly dependent on the model determination of the total downwelling irradiance. Figure 12 indicates the accuracy of this determination by comparing the calculated and measured irradiances for two times within the experiment windows.)

Figure 13 shows the comparison between the surface reflectances calculated using the nadir value of the remote sensor data from three altitudes and that measured by Scripps at the water surface. The calculated surface reflectances are the averages from three overflights at each altitude. It is evident that the best agreement is realized for an altitude of 152 m where the effects of the atmosphere are small. And since the contribution from specular reflectance is significant at this altitude and less so at higher altitudes, the comparison indicates a need for some improvement in the correction for atmospheric scattering.

To determine the effect of the various input variables on the calculated surface reflectance, a parametric analysis was performed. Each variable was changed by some reasonable percentage from its best measured or best estimated value and used with the 12.5 km data. The resulting percent changes in the calculated surface reflectance are shown in table II. It should be noted that the magnitude of the parametric changes is very specific to the reference values about which the changes are made. A complete parametric analysis therefore should include additional reference conditions such as water with higher concentrations of contaminants or an atmosphere having a greater level of haze. It is evident, however, that small changes in a combination of parameters could account for the errors in the comparison shown in figure 13.

Another dimension of the atmospheric scattering model that must be considered, is its ability to correct for limb brightening, i.e., the increase in aperture radiance as a function of look angle. Figures 14 and 15 show the comparison of the measured and calculated radiance as a function of look angle for an altitude of 152 m and 12.5 km. The calculated radiance was determined assuming the surface radiance and the specular reflectance to be independent of look angle. All of the calculated limb brightening is thus provided by the model. As can be seen the calculated limb brightening is much lower than measured. A parametric analysis indicated that no change in any one or a combination of input variables could account for this difference. To establish the cause of this difference will require a better understanding of the angular dependence of the upwelling surface radiance, the specular reflectance and/or the diffuse sky radiance.

SUMMARY OF RESULTS

The purpose of this experiment was to assess the accuracy of atmospheric corrections to remotely sensed multispectral scanner data through use of the subject radiative transfer model. The conclusions resulting from this assessment are as follows:

1. At an altitude of 152 m (500 ft) where the contribution from the atmosphere was not a factor, the surface measured radiance was consistently lower (about one-half) than the remotely measured radiance. The difference in the measured values was attributed to specular reflectance of skylight at the water surface.

2. For the conditions reported here, the specular reflectance was determined to be 2% which is consistent with accepted values. Therefore, the calculated radiance at altitude was increased by an amount dependent on this percentage, the altitude and the calculated sky irradiance. The radiance thus calculated agreed to within 14% and 16% for sensor altitudes of 15.2 km (41,000 ft) and 152 m (500 ft) respectively.

3. The surface reflectance calculated using the remote sensor data measured at an altitude of 152 m compared well with that measured at the surface by Scripps. (Here surface reflectance is the ratio of the irradiance above the surface due to upwelling from below the water surface and the total downwelling irradiance above the surface.) However, the calculated reflectance increased as the sensor altitude increased. Small errors in a combination of atmospheric scattering model input variables could account for these increases.

4. The remotely measured radiance compares poorly with the calculated radiance as a function of look angle. There is a strong indication that no change or combination of changes in the model input variable will account for this discrepancy.

5. An accurate assessment of the corrections for atmospheric effects provided by the radiative transfer model cannot be made without a better understanding of the contributions made by the air-water interface, the sea state, and the sky radiance. Additionally the assessment should be made using data from both high and low concentrations of chlorophyll and/or suspended solids in the water.

REFERENCES

1. Morel, A. and Prieur, L.: Analysis of Variation in Ocean Color. Limnol. Oceanogr., vol. 22, no. 4, July 1977, pp. 709-722.
2. Miller, J. R.; et al.: Interpretation of Airborne Spectral Reflectance Measurements Over Georgian Bay. Remote Sensing of Environment, vol. 6, no. 3, 1977, pp. 183-200.
3. Mueller, J. L.; Ball, D. L.; and Middleton, E. M.: Parametrization and Pre-Processing of Ocean Color Image Data for Studies of Coastal Oceanography. Ninth Annual Offshore Technology Conference, AIME, 1977, Paper OTC-2761, pp. 295-302.
4. Gordon, H. R.: Removal of Atmospheric Effects from Satellite Imagery of the Oceans. Appl. Opt., vol. 17, no. 5, May 1978, pp. 1631-1636.
5. Turner, R. E.: Atmospheric Transformation of Multispectral Remote Sensor Data. (ERIM-12-6100-3-F, Environmental Research Inst. of Michigan; NASA Contract NAS3-20483.) NASA CR-135338, 1977.
6. Standard Methods for the Examination of Water and Wastewater. Fourteenth ed. American Public Health Assoc., 1976.

7. Duntley, S. Q.; et al.: Ocean Color Analysis. SIO-REF-74-10, Scripps Institution of Oceanography, 1974, pp. 2-1 to 2-18.

Table I. Input Variables

Estimated	Measured
Extraterrestrial solar irradiance	Date
Barometric pressure at sensor altitude	Time
Background albedo	Experiment site latitude and longitude
Haze type and refractive index	Sensor and site altitudes
Ozone column density	Surface barometric pressure
Ratio of aerosol scattering optical thickness to total aerosol optical thickness	Sensor center wavelengths
Optical depth above 5 km	Optical thickness as a function of wavelength
	Angle of the scan plane

Table II. Sample Parametric Analysis Using the Atmospheric Scattering Model

Input variable	Change in input variable, percent*	Resulting change in calculated reflectance, percent			
		425 nm	502 nm	591 nm	672 nm
Measured radiance at 12.5 km	+10	+81	+48	+21	+65
Skylight reflectance	+50	-12	-12	-6	-35
Time	-6 min (from 0915 hr)	+17	+8	+5	+7
Optical thickness	+20	-46	-42	-24	-88
Altitude	-1	+2	+1	+1	0
Background albedo	-50	+91	+19	+6	+37
Barometric pressure at altitude	+20	+13	+4	+1	0
Refractive index	1.5 - 0.1 i (from Haze M 1.5 - 0 i)	+117	+14	+5	+42
Haze type	Haze L (from Haze M)	-4	-4	-2	-9
Difference in measured reflectance for a sensor altitude of 12.5 km as compared with the reflectance measured at the surface, percent		+462	+35	+112	+115

*Unless otherwise noted.

Figure 1. F 106 high altitude aircraft - platform for Ocean Color Scanner.

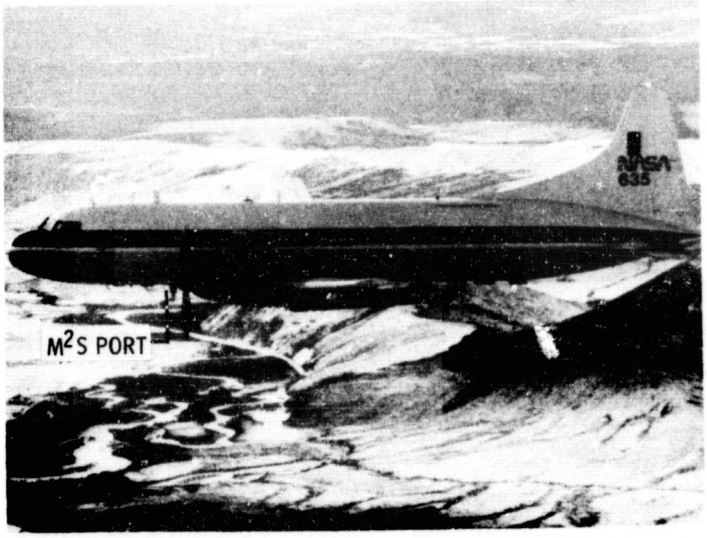

Figure 2. C 131 medium altitude aircraft - platform for modular multispectral scanner.

Figure 3. R/V Crockett - platform for surface truth instrumentation.

Figure 4. Scripps Institute of Oceanography's submersible spectroradiometer.

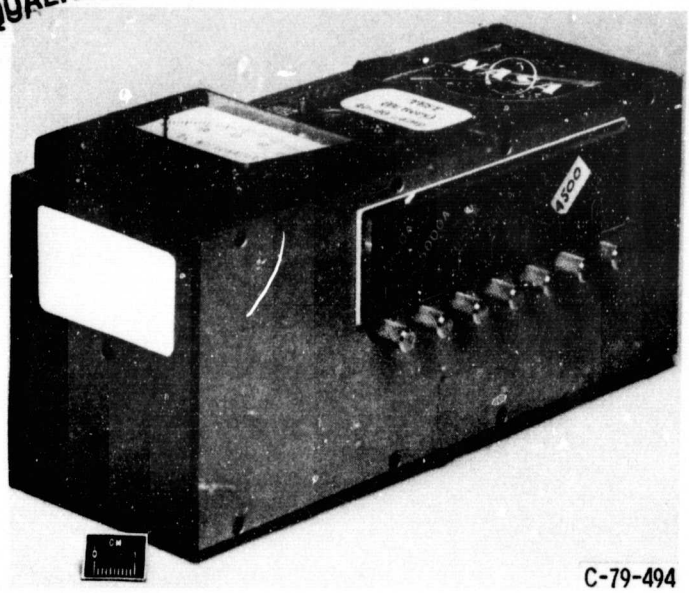

Figure 5. Seven band solar radiometer.

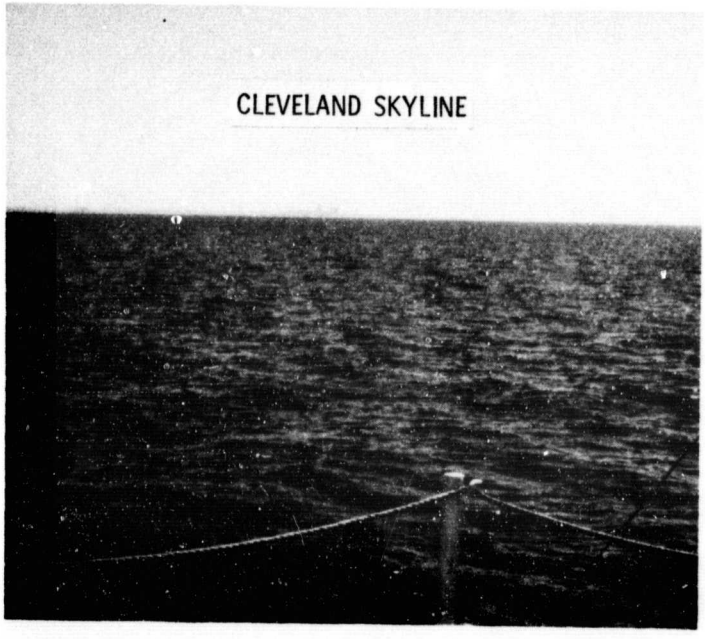

Figure 6. Typical sea and atmospheric state on June 22, 1978 at experiment site.

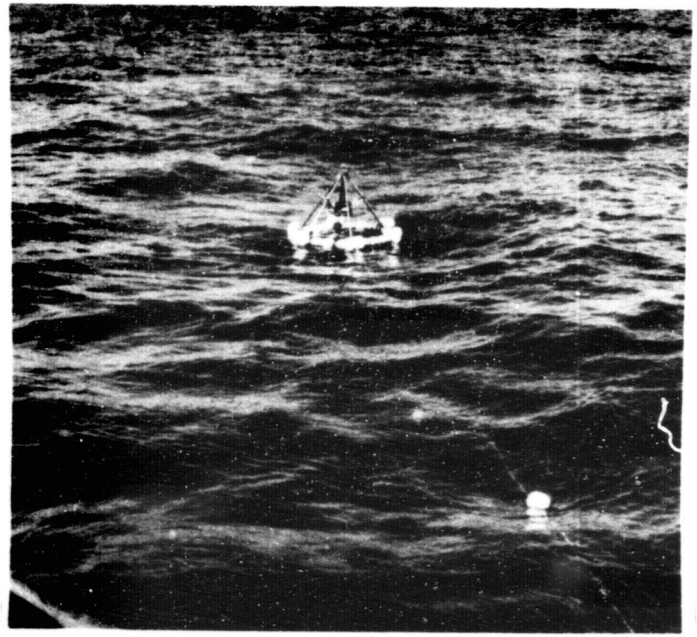

Figure 7. Spectroradiometer deployed under support float 30 meters from ship.

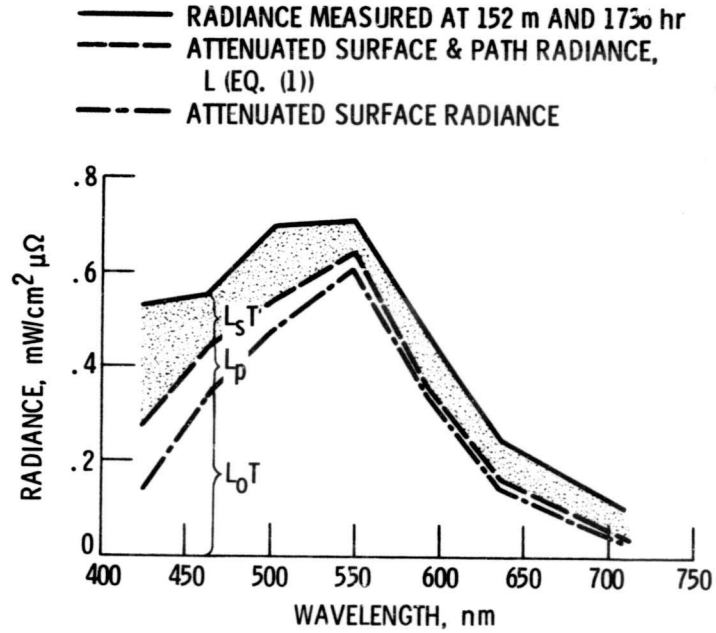

Figure 8. - Illustration of three components of measured radiance, i.e., specularly reflected skylight (L_sT), path radiance (L_p), and surface radiance (L_oT) for a sensor altitude of 152 m.

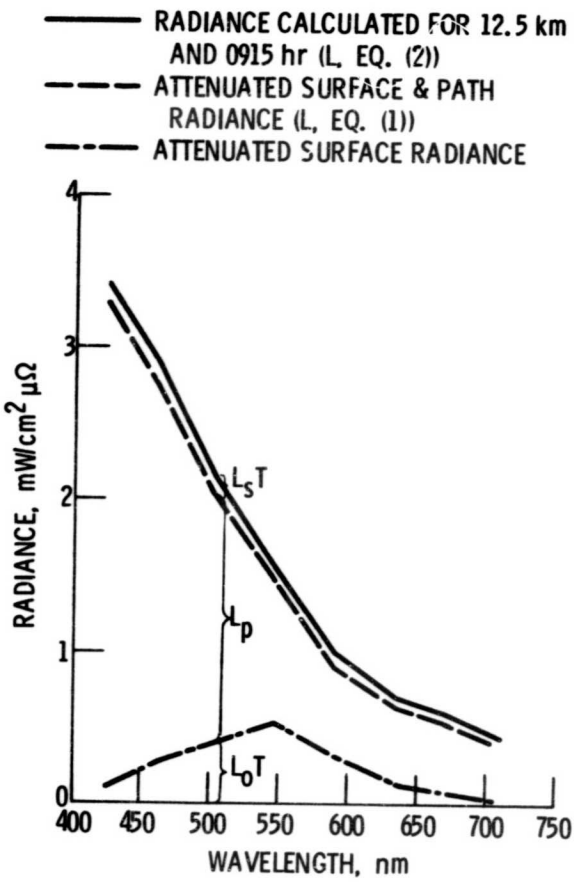

Figure 9. - Relative magnitude of the three components of calculated radiance for a sensor altitude of 12.5 km.

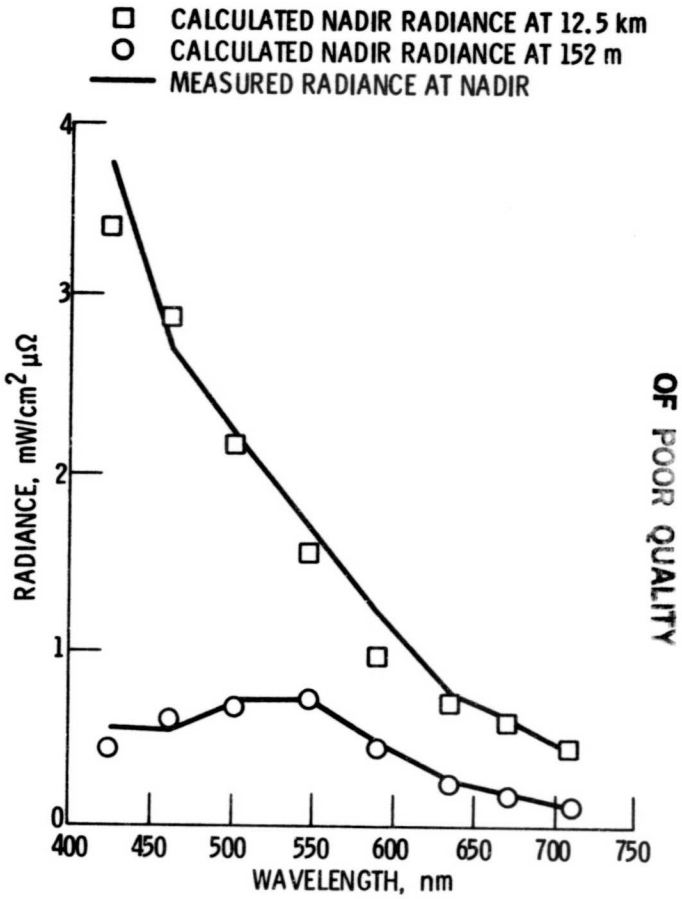

Figure 10. - Comparison of measured and calculated nadir radiance at 12.5 km and 152 m for a solar zenith angle at 55°.

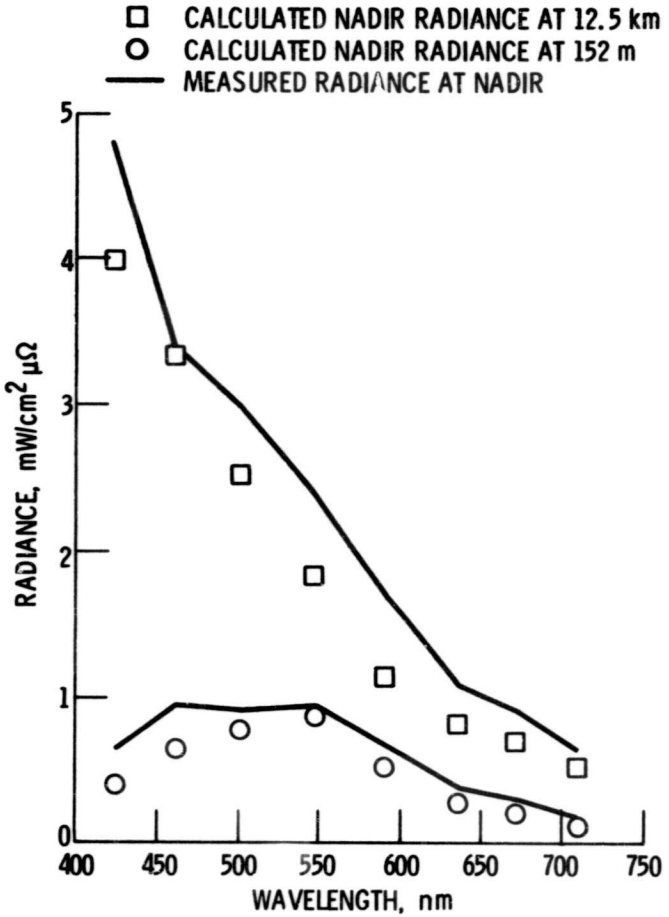

Figure 11. - Comparison of measured and calculated nadir radiance at 12.5 km and 152 m for a solar zenith angle at 44°.

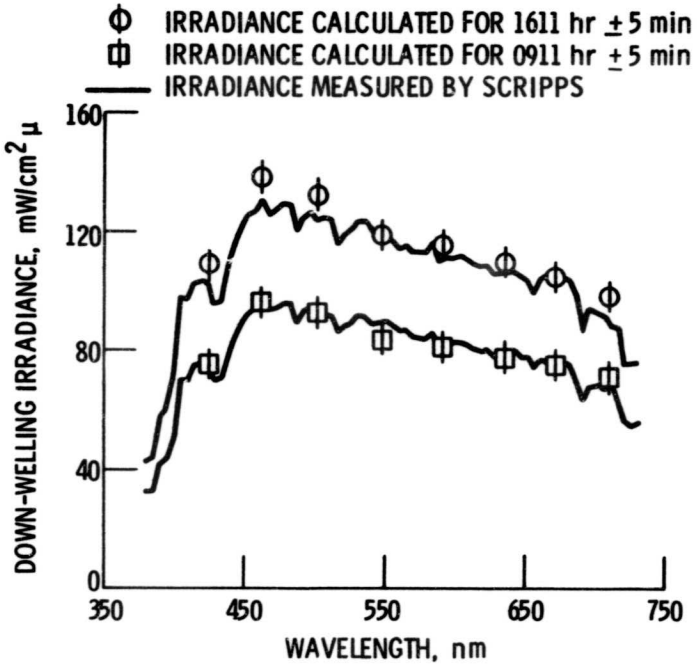

Figure 12. - Comparison of measured and calculated down-welling irradiance at 0911 and 1611 hours.

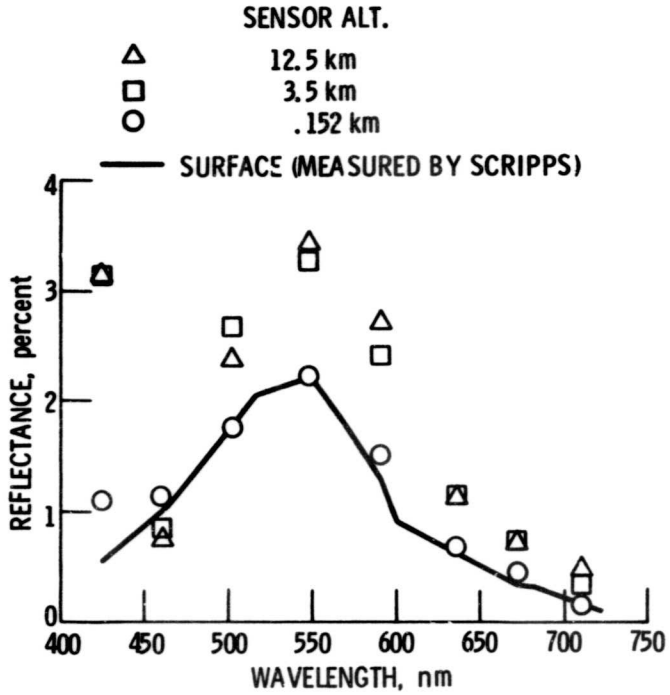

Figure 13. - Average measured reflectance as a function of sensor altitude compared with reflectance measured on the water surface.

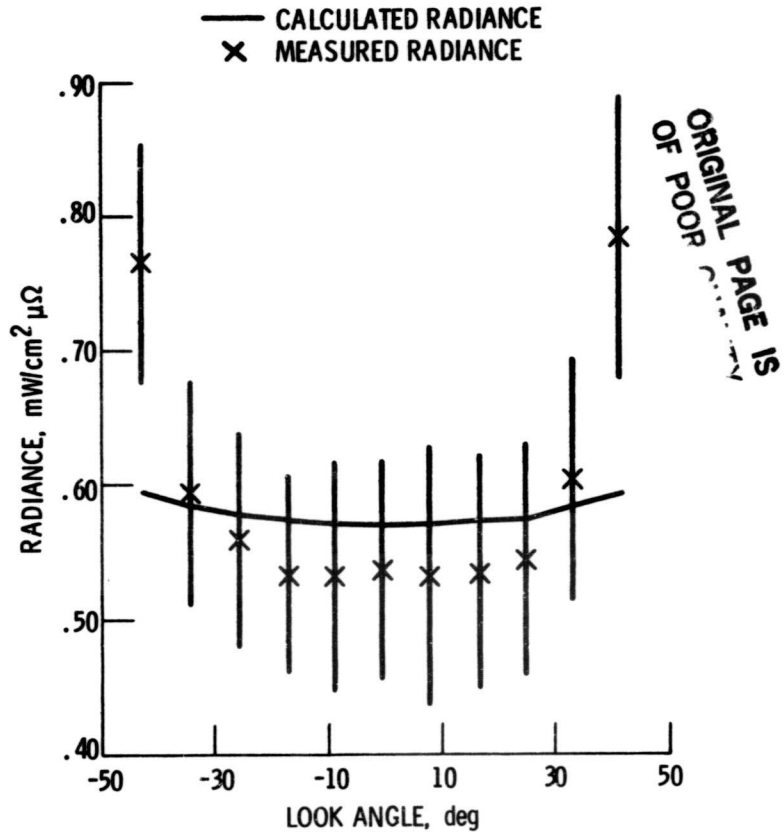

Figure 14. - Comparison of measured and calculated radiance as a function of look angle for a sensor altitude of 152 m, a wavelength of 462 nm and a time of 1015 hr.

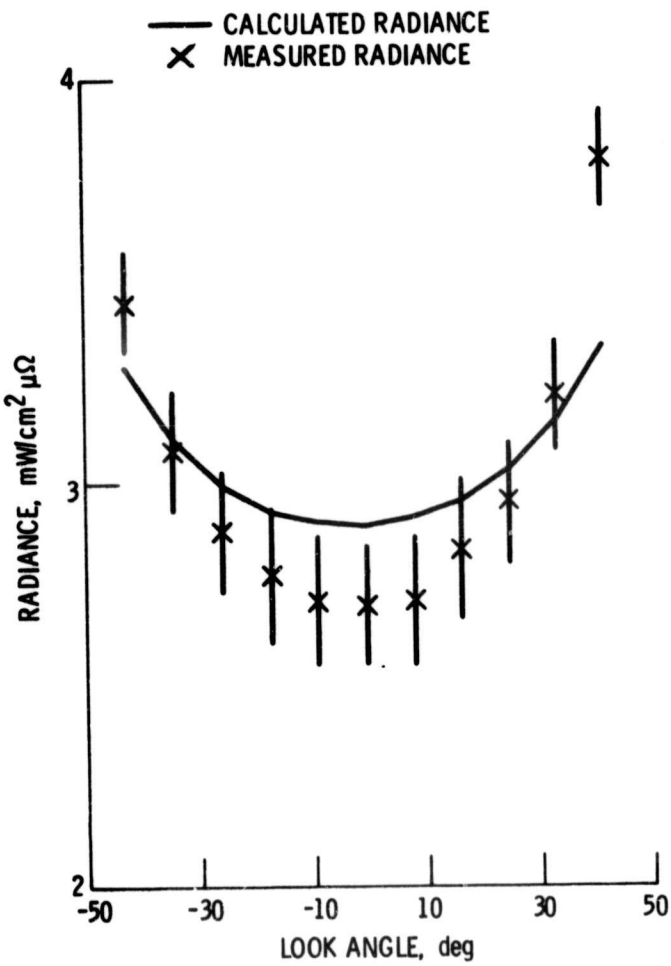

Figure 15. - Comparison of measured and calculated radiance as a function of look angle for a sensor altitude of 12.5 km, a wavelength of 462 nm and a time of 0915 hr.